Trends in electrical transport of *p*-type skutterudites RFe_4Sb_{12} (R = Na, K, Ca, Sr, Ba, La, Ce, Pr, Yb) from first-principles calculations and Boltzmann transport theory

Jiong Yang, P. Qiu, R. Liu, L. Xi, S. Zheng, W. Zhang,* and L. Chen
State Key Laboratory of High Performance Ceramics and Superfine Microstructure, Shanghai Institute of Ceramics, Chinese Academy of Sciences, Shanghai 200050, China

D. J. Singh
Materials Science and Technology Division, Oak Ridge National Laboratory, Oak Ridge, Tennessee 37831-6114, USA

Jihui Yang
Materials Science and Engineering Department, University of Washington, Seattle, Washington 98195-2120, USA
(Received 14 July 2011; revised manuscript received 9 October 2011; published 6 December 2011)

We report a consistent set of *ab initio* calculations of the electronic structures and electrical transport properties of *p*-type thermoelectric compounds RFe_4Sb_{12}, where R is a rattling filler selected from alkali metals (Na, K), alkaline earths (Ca, Sr, Ba), and rare earth metals (La, Ce, Pr, Yb). Different from the single Sb-dominated light band in the valence band edge of $CoSb_3$, the heavy bands from Fe d electronic states also fall in the energy range close to the valence band edges in the RFe_4Sb_{12}. These heavy bands dominate the band-edge density of states, pin the Fermi levels, and mostly determine the electrical transport properties of those *p*-type RFe_4Sb_{12}. The Seebeck coefficients can be roughly categorized into three groups based on the charge states of fillers, and the maxima are lower than those of *n*-type $CoSb_3$ skutterudites. Effective carrier relaxation time in *p*-type RFe_4Sb_{12}, obtained from the combinations of calculations and experiments, is remarkably similar among different compounds with values around 7.5×10^{-15} s and weak temperature dependence. The optimal doping levels of those RFe_4Sb_{12} are estimated to be around 0.6–0.8 holes per unit cell at 850 K, which is difficult to achieve in RFe_4Sb_{12} compounds. Prospects for further improving the performance of *p*-type skutterudites are also discussed.

DOI: 10.1103/PhysRevB.84.235205 PACS number(s): 72.15.Jf, 71.20.Nr, 71.28.+d

I. INTRODUCTION

Skutterudites were recognized as potential high-performance thermoelectric (TE) materials in the middle of 1990s.[1–3] Binary skutterudites, such as $CoSb_3$, crystallize with a body-centered-cubic structure, space group $Im3$, and a primitive unit cell containing four formula units, i.e. Co_4Sb_{12}. This structure contains a large void site, coordinated by Sb, which can be partially filled with electropositive ions. The binary compounds generally form as *p*-type semiconductors and show high carrier mobilities.[3] While this structure type is common and occurs for a variety of pnictogen and transition metal elements, we focus here on Co and Fe antimonides because of their practical importance in thermoelectrics.

Filling the voids in the ideal binary structure with electropositive elements to produce so-called filled skutterudites has proved to be an effective way to improve the TE performance with both *n*-type and *p*-type compositions. These filled materials have much lower lattice thermal conductivities than the binary compounds.[2] The reduction in lattice thermal conductivity plays a central role in improving the thermoelectric performance of these materials, as characterized by the figure of merit $ZT = \sigma S^2 T/\kappa$, where σ is the electrical conductivity, κ ($=\kappa_e + \kappa_L$) is the thermal conductivity written as the sum of electronic and lattice components, T is temperature, and S is the Seebeck coefficient, also called the thermopower.

Many of the rare-earths (RE), alkaline-earths (AE), and alkali metals (AM) have been confirmed to fill into the crystal voids of $CoSb_3$,[4–12] to form $R_xCo_4Sb_{12}$, as predicted by a rule based on electronegativity as proposed by Shi *et al.*[13] The best figure of merit values of *n*-type $CoSb_3$ skutterudites reach 1.7,[14] which makes the filled $CoSb_3$-based skutterudites among the most promising bulk TE materials for power generation applications. Both experiments and theoretical calculations indicate that the band-edge electronic structures of *n*-type filled $CoSb_3$ skutterudites are almost unaffected by fillers, at least for moderate filling fraction x, and that the optimal doping levels for the maximum power factors $S^2\sigma$ (over 50 μV/cm-K^2) fall in the range of 0.4–0.6 electrons per Co_4Sb_{12} cell.[14–16] Recent work also demonstrated that multiple fillers can further scatter the heat-conducting lattice phonons with frequencies close to the vibrational modes of fillers and minimize κ_L.[14,16–19] The synergetic optimization of the electrical and thermal transport leads to an increase in maximum ZT values, going from single to multiple filling in *n*-type $CoSb_3$.[14]

Thermoelectric modules consist of legs of *p*-type and *n*-type materials. It is highly desirable for reasons of mechanical integrity and performance that the materials used for the p and n legs in a given module possess similar thermomechanical properties and close enough ZT values for maximum efficiency. That is, to realize the potential of the high ZT in *n*-type skutterudites, it will be necessary to have similar performing *p*-type skutterudites. However, Fe-based *p*-type filled skutterudites have been studied for more than 15 years, and the maximum ZT values barely exceed unity in the best cases.[1,2,20–24] The purpose of this paper is to examine trends in the properties of these *p*-type materials to obtain better understanding of the fundamental factors limiting performance.

The doping of skutterudites may be understood within a Zintl concept. The electropositive filler atoms donate electrons to the transition metal-antimony framework which obeys an electron counting rule. Fe has one fewer electron than Co; therefore, the achievable filling fractions x in Fe-based p-type skutterudites are much higher than those in n-type Co-based skutterudites. As mentioned, filler atoms greatly reduce the thermal conductivity; thus, the filled Fe-based skutterudites have relatively low κ_L. Therefore the performance asymmetry between the best known n-type and p-type filled skutterudites has its origin in the electrical transport.

The fully filled $R\mathrm{Fe_4Sb_{12}}$ skutterudites exhibit many interesting low-temperature physical properties, including magnetism, quantum critical behavior, and both conventional electron-phonon and unconventional superconductivity depending on compounds.[25–33] As for the high-temperature TE properties, they also have the highest power factors among the p-type skutterudites, around 30–35 μV/cm-K^2 in our previous study.[24] Their ZT values have reached nearly 1.0 with composition optimization, but these power factors are still lower than those of n-type skutterudites.

The first key concern in this study is how the filler and Fe atoms affect the valence bands (VBs), which are critical for p-type electrical transport. Since the TE $R_x\mathrm{Fe_4Sb_{12}}$ are almost fully filled, the effect of the fillers on the electronic structures is expected to be stronger than that in the partially filled $R_x\mathrm{Co_4Sb_{12}}$ compounds. Furthermore, the replacement of Co by Fe may also alter the VBs. Besides the electronic structures, the study of electrical transport properties is also important, for example, to identify the optimal doping levels and to understand why the power factors of the p-type skutterudites are lower than those of the n-type materials.

II. THEORETICAL METHODS

Our first-principles calculations were performed with the generalized gradient approximation (GGA) functional of Perdew, Burke, and Ernzerhof (PBE),[34] with projected augmented wave (PAW) method,[35,36] as implemented in Vienna *ab initio* simulation package (VASP).[37] We set the plane-wave cutoff to 300 eV for all $R\mathrm{Fe_4Sb_{12}}$ systems. Since the filling fractions of $R\mathrm{Fe_4Sb_{12}}$ skutterudites are close to 100% and one of the goals of this study is to separate the intrinsic trends with the identity of the filler atoms R, we adopt a fully filled 17-atom unit cell in the calculations. Filler atoms R were selected from alkali metals (Na, K), alkaline earth metals (Ca, Sr, Ba), and rare earth metals (La, Ce, Pr, Yb), covering most of the stable fillers. Lattice constants and internal atomic coordinates were fully relaxed by total energy minimization. The electronic structures used in the transport calculations were obtained based on these resulting lattice structures.

We then used Boltzmann transport theory with the constant relaxation time approximation to obtain electrical transport properties, including Seebeck coefficients, electrical conductivities, and power factors. An important feature of this method is that the Seebeck coefficient as a function of temperature can be obtained directly with no adjustable parameters. This has proven valuable in studying a number of useful TE materials and has yielded predictions that have been confirmed by subsequent experiments.[38–42] Details of the methodology are given in Refs. 40–42. A key quantity for electrical transport is the electronic group velocity, $\mathbf{v}_{i,\mathbf{k}} = \frac{1}{\hbar}\nabla_{\mathbf{k}}\varepsilon_{i,\mathbf{k}}$, where the $\varepsilon_{i,\mathbf{k}}$ is the band energy. These can be evaluated directly using fits or interpolations of the bands or via the momentum matrix elements. Here, the velocities were calculated with momentum matrix method: $\mathbf{v}_{i,\mathbf{k}} = \frac{1}{m_e}\langle\Psi_{i,\mathbf{k}}|\hat{\mathbf{p}}|\Psi_{i,\mathbf{k}}\rangle$, where m_e and i are the mass of electron and band index, respectively. We used $21 \times 21 \times 21$ Monkhorst–Pack $\mathbf{k}$-point samplings[43] in the Brillouin zones, which provides well-converged electronic transport quantities. Spin orbit is not included in our calculations since it is only a minor reduction in the thermopower, particularly for low doping levels, as discussed in Ref. 44. $R\mathrm{Fe_4Sb_{12}}$ in this paper, on the other hand, are all heavily doped semiconductors; and minor change in thermopower will not alter the physical trend in our synergetic study.

The filled $R\mathrm{Fe_4Sb_{12}}$ compounds show interesting magnetic behavior at low temperature, with a clear trend based on electron count.[25–30] The alkali metal filled skutterudites are ferromagnetic at low temperature [$\sim$80 K for $\mathrm{NaFe_4Sb_{12}}$ and $\mathrm{KFe_4Sb_{12}}$ (Ref. 30)], and the alkaline earth filled materials are paramagnets apparently near ferromagnetism. Eu^{2+} filling yields unusual ferromagnetism related to the interaction of a nearly ferromagnetic host with Eu^{2+} moments,[25] while filling with trivalent rare earths yields ordinary paramagnetism. These behaviors reflect the effect in the Stoner theory of magnetism[45] from the increase in the density of states as the electron count in $R\mathrm{Fe_4Sb_{12}}$ is lowered going from trivalent rare earth to divalent and finally monovalent fillers. This is associated with the narrow Fe derived bands below the valence band maximum (VBM), which are also thought to be of importance for the thermoelectric behavior.[44,46] Since we are interested in compounds that are effectively itinerant metals that either do not order or have magnetic orderings well below the temperature range that we consider, we adopt the standard approach in Boltzmann theory, which is to use the nonspin-polarized electronic structure to define the carriers and consider the spin fluctuations as sources of scattering.

Another issue related to calculations is how to treat the f electrons of rare earth fillers. Density functional calculations showed that the charge state of Ce in skutterudites is +3,[47] as was confirmed in experiments.[48] Nouneh *et al.* measured the Seebeck coefficients of $\mathrm{CeFe_4Sb_{12}}$ and $\mathrm{LaFe_4Sb_{12}}$ from 0 to 400 K, finding that they became comparable above about 150 K and were almost the same above 400 K.[49] That means the Ce f electrons could not play a role in the electronic structure relevant to transport. In our experiments, we found that the low-temperature transport properties vary with rare earth filler atoms, which may stem from Kondo effect.[50] However, above room temperature, $R\mathrm{Fe_4Sb_{12}}$ with filler atoms from La to Nd, i.e. different numbers of f electrons, show very similar temperature dependences of σ and S. Therefore, we regard the f electrons as localized and corelike orbitals and treat them as frozen core electrons for the construction of the PAW potentials in the present calculations. While this appears to be appropriate for the high-temperature transport properties, we expect that calculations with f electron states as well as spin polarization are needed for addressing the low-temperature properties of systems such as $\mathrm{CeFe_4Sb_{12}}$ and $\mathrm{EuFe_4Sb_{12}}$, as has also been noted previously.[51]

III. STRUCTURAL PROPERTIES AND ELECTRONIC STRUCTURES

In Table I, structural properties of all RFe$_4$Sb$_{12}$, including lattice constants, atomic coordinates, and interatomic distances, have been presented. Experimental results are listed for comparison.[24,30–33] The structure of RFe$_4$Sb$_{12}$ is in the type of LaFe$_4$P$_{12}$. In the conventional cell, R is in 2a position (0, 0, 0), and Fe is in 8c (0.25, 0.25, 0.25). There are two dimensionless internal parameters specifying the coordinates of Sb atoms, as shown in Table I. The largest deviations from available experimental coordinates of Sb are within 2–3%, which are reasonably well. Our lattice constants are all slightly larger than experimental counterparts, within 0.1–0.5 percentages, which is acceptable considering the overestimations of lattice constants by using GGA and possible deficiency of fillers in experiments. In AM- and AE-filled RFe$_4$Sb$_{12}$, the lattice constants as well as the interatomic distances are clearly related with the radii of fillers, getting enlarged along with the size of fillers. Since the filling fractions in RFe$_4$Sb$_{12}$ are close to unity, the structural variations caused by fillers are larger than those in n-type skutterudites and will have influences on their band structures (see below). La-, Ce-, Pr-filled RFe$_4$Sb$_{12}$ have similar structural parameters, and their lattice constants are all smaller than other RFe$_4$Sb$_{12}$, both theoretically and experimentally. YbFe$_4$Sb$_{12}$ and CaFe$_4$Sb$_{12}$ possess close enough structural parameters in our calculations and may result in similar electronic properties.

To address the general feature of the electronic structures of RFe$_4$Sb$_{12}$, we first present the projected band structures around the Fermi level of the typical p-type skutterudite BaFe$_4$Sb$_{12}$, in the energy range −1.5 to 1.5 eV [Figs. 1(a)–1(b)]. As expected, the role of Ba is to donate electrons to the Fe$_4$Sb$_{12}$ framework and modify the band structure through its impacts on other framework atoms, as in a typical Zintl type material. Since Ba itself contributes little to the bands in this range, here we only give the projected band structures from Fe and Sb. For comparison, the projected band structures onto the transition metal (TM) site for Co$_4$Sb$_{12}$ are also shown [Fig. 1(c)].

The VB of Co$_4$Sb$_{12}$ shows a gap-crossing light band with a quasilinear dispersion around Γ point as noted in prior work.[52–54] The light band has stronger Sb p character, though it hybridizes with Co. Since there is only one single light band at the top of the VB, it is not favorable for high p-type Seebeck coefficients, at least for doping levels where the Fermi levels remains above the top of the heavy bands. Similar to Co$_4$Sb$_{12}$, the light band of BaFe$_4$Sb$_{12}$ possesses a region with a quasilinear dispersion away from band maximum at the Γ point. In both compounds, the light band forms the VBM and is followed by several heavy bands with large TM d projections (though they are hybridized with Sb) at higher binding energy. The spatially localized nature of 3d orbitals is the reason for large effective masses of these heavy bands. In contrast, Ir$_4$Sb$_{12}$, which is the corresponding 5d compound, shows broader bands in this energy range.[52] The major difference in VB between Co$_4$Sb$_{12}$ and BaFe$_4$Sb$_{12}$ is the energy difference between light band and heavy bands at Γ point (labeled as Δ_0 for the convenience of discussion), which is 0.64 eV in Co$_4$Sb$_{12}$ and 0.25 eV in BaFe$_4$Sb$_{12}$. Singh also reported a light band upward shift relative to flat bands as Co concentration increases in La(Fe, Co)$_4$Sb$_{12}$.[51]

The band structures of Co$_4$Sb$_{12}$ and BaFe$_4$Sb$_{12}$ have a strong asymmetry between holes and electrons. The conduction bands (CBs) of the two skutterudite compounds are also primarily composed of d orbitals from TMs, as shown in Figs. 1(a)–1(c), while Sb p states have some contributions through p-d hybridization. Several heavy bands making up the region near the conduction band minimum is the reason for the high Seebeck coefficients seen at relatively high carrier concentration when Co$_4$Sb$_{12}$ becomes n type. Both of them have direct band gaps at Γ point. The gap value is 0.49 eV for BaFe$_4$Sb$_{12}$, obviously larger than that of Co$_4$Sb$_{12}$, which is 0.17 eV in our calculation. The 0.17 eV gap result of Co$_4$Sb$_{12}$ agrees very well with the result of Sofo *et al.*, who adopted linearized augmented plane-wave (LAPW) method and GGA exchange-correlation functional.[55]

TABLE I. Crystallographic properties of RFe$_4$Sb$_{12}$, R = Na, K, Ca, Sr, Ba, La, Ce, Pr, Yb. R is in 2a (0, 0, 0); Fe in 8c (1/4, 1/4, 1/4); Sb in 24g(0, y, z).

	Lattice constants (Å)		Coordinates of Sb (0, y, z)				Interatomic distances (Å)	
R	a	a_{exp}	y	z	y_{exp}	z_{exp}	R-Sb	Fe-Sb
Na[a]	9.1846	9.1767	0.1620	0.3329	0.1588	0.3369	3.400	2.550
K[a]	9.2200	9.1994	0.1641	0.3369			3.455	2.566
Ca[b]	9.1854	9.1631	0.1626	0.3342	0.1596	0.3367	3.414	2.553
Sr[b]	9.2029	9.1810	0.1640	0.3347	0.1600	0.3380	3.447	2.561
Ba[b]	9.2470	9.2058	0.1654	0.3385	0.1613	0.3402	3.481	2.572
La[b]	9.1769	9.1454	0.1635	0.3352			3.422	2.550
Ce[c]	9.1828	9.140	0.1633	0.3353			3.425	2.553
Pr[d]	9.1792	9.1369	0.1630	0.3347	0.1598	0.3348	3.418	2.551
Yb[e]	9.1853	9.1586	0.1623	0.3337	0.1637	0.3403	3.405	2.549

[a]Reference 31.
[b]Reference 30.
[c]Reference 24.
[d]Reference 32.
[e]Reference 33.

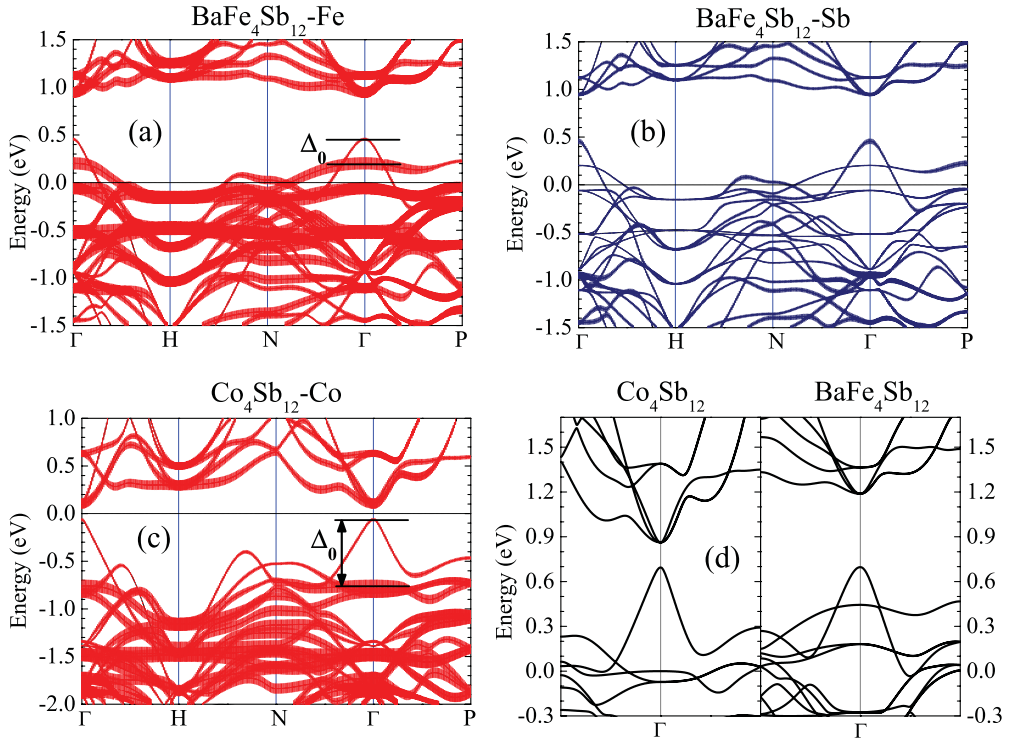

FIG. 1. (Color online) Partial band structures of $BaFe_4Sb_{12}$ projected on (a) Fe, (b) Sb, and (c) Co_4Sb_{12} projected on Co. Vertical bars superimposed on band structures represent the strength of band characters from certain atomic states. The aligned bands of $CoSb_3$ and $BaFe_4Sb_{12}$ based on the 1*s* orbitals of Sb are shown in (d).

All-electron band alignment calculations have been done in order to address the problem why the band gap becomes larger and why Δ_0 shifts in $BaFe_4Sb_{12}$ as well as in other RFe_4Sb_{12}. These band alignment calculations allow us to reveal the effect of changes in the Coulomb potential due to difference chemical circumstances. We take the 1*s* states of Sb as a reference level, which do not participate in bonding but do respond to shifts in the electrostatic potential. The band alignment calculations were carried out using the WIEN2k package,[56] in which the energy levels of core states can be easily obtained. The reliability of taking core states as reference levels in WIEN2k has been testified by previous deformation potential calculations, as shown in Refs. 57 and 58. The aligned band structures in the vicinity of Γ point with this reference level are shown in Fig. 1(d). The heavy bands in VB, as well as the whole CB, shift upwards by 0.43 eV in $BaFe_4Sb_{12}$ comparing with the corresponding bands in Co_4Sb_{12}. The light Sb band forming the VBM, on the other hand, shifts very little in the two compounds. Band alignments of the other RFe_4Sb_{12} have also been investigated with fillers R = Na, K, Ca, La. Although the values of Δ_0 fluctuate in an energy range of 0.30 eV (0.21 eV for Na, 0.31 eV for K, 0.19 eV for Ca, and 0.01 eV for La), the energy positions of the heavy bands in VB, as well as the whole CB at Γ point, are almost fixed in these RFe_4Sb_{12}, since these bands are primarily determined by Fe atoms. The heavy bands in RFe_4Sb_{12} are much closer to the VBM comparing with *n*-type $CoSb_3$ skutterudites, and this feature is crucial for the *p*-type electrical transport. Also, the relatively large band gaps that are opened by filling imply that bipolar effects on the *p*-type electrical transport will be negligible in the RFe_4Sb_{12} compounds at achievable temperatures.

Figure 2 plots the band structures of all the RFe_4Sb_{12} investigated. The charge states of the filler atoms are +1 for Na and K, +2 for Ca, Sr, Ba, and Yb, and +3 for La, Ce, and Pr. The band gaps of RFe_4Sb_{12} are all larger compared with that of *n*-type $CoSb_3$ for the reason discussed above. As in $BaFe_4Sb_{12}$, the coexistence of single light band and multiple heavy bands around VBM appears in all the RFe_4Sb_{12}. The heavy bands are so flat that the Fermi levels are almost pinned in them. The Fermi levels of $BaFe_4Sb_{12}$ at both 300 and 850 K are marked in Fig. 2(d). It moves upwards only by 0.02 eV going from 300 to 850 K, and still lies in the heavy bands.

Unlike the case in *n*-type skutterudites,[14,15] fillers in RFe_4Sb_{12} do affect some band details due to their extremely high filling fractions, including Δ_0, the shape of CB minima, and some band variations in VB. Take Ca-, Sr-, and Ba-filled RFe_4Sb_{12} as examples. We found that, under the same divalent charge state, Δ_0 increases with the size of fillers, from 0.19 eV for $CaFe_4Sb_{12}$, 0.23 eV for $SrFe_4Sb_{12}$, and 0.25 eV for $BaFe_4Sb_{12}$. Band alignment results show that the difference comes from the shift of the light band maximum, and the energy positions of the heavy bands are almost unchanged, as mentioned above. Another distinct difference in VB among the three divalent fillings is the top bands at P point, which are split in $BaFe_4Sb_{12}$, but not the case in $CaFe_4Sb_{12}$. The changes around CB minima turn the bands from indirect ($CaFe_4Sb_{12}$) to direct Γ-Γ ($BaFe_4Sb_{12}$) gaps. It should be noted that, in

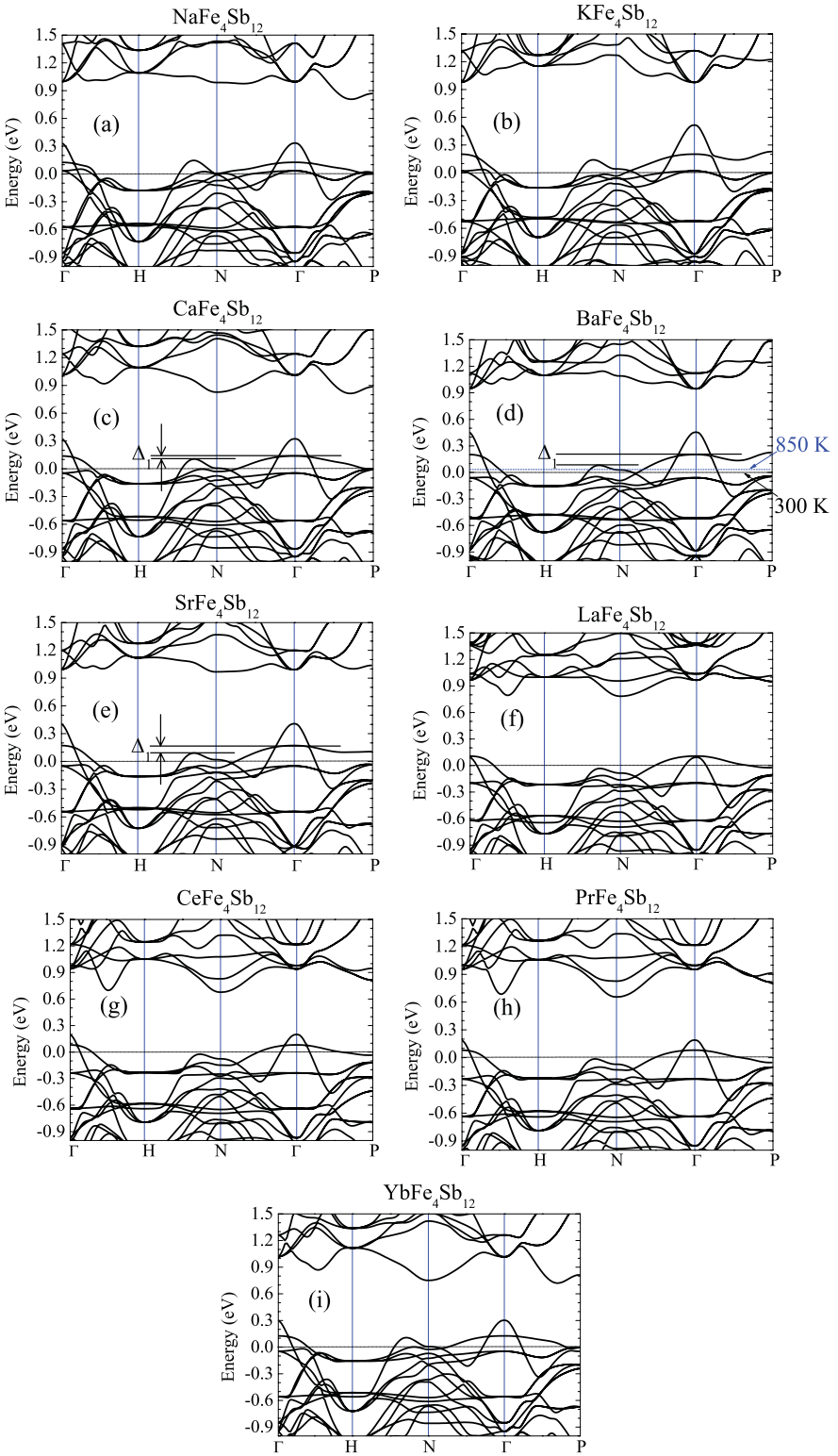

FIG. 2. (Color online) Band structures for RFe$_4$Sb$_{12}$ (R = Na, K, Ca, Ba, Sr, La, Ce, Pr, and Yb). Zero energy points are the Fermi levels at 300 K for all these compounds.

the energy space, the maximum electronic states along the H → N at VB are close to the heavy bands at the Γ point. The difference between the maximum energy along H → N and the heavy band maximum at the Γ point, denoted by Δ_1 in Fig. 2, is 0.03 eV for CaFe$_4$Sb$_{12}$, 0.08 eV for SrFe$_4$Sb$_{12}$, and 0.12 eV for BaFe$_4$Sb$_{12}$ [Figs. 2(c)–2(e)]. Since the degeneracy of k points along H → N is higher than k points along other high symmetrical lines (such as N → Γ and Γ → P), energy states on these k points will serve as hole pockets and contribute to the DOS more effectively. Small Δ_1 means energy states of k points along H → N are close to the onset of heavy bands, thus is expected to increase the slope of DOS at the VB edge. As discussed before, the band structure is sensitive to the positions of the Sb atoms surrounding the filler;[1,55,59] therefore, it is not surprising that the energy positions of some bands containing Sb contributions [Fig. 1(b)] are sensitive to

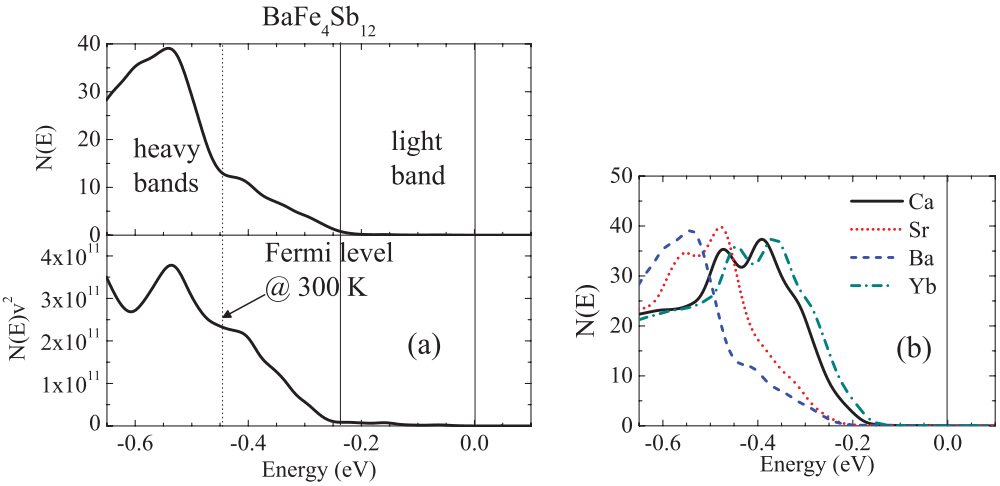

FIG. 3. (Color online) (a) Density of states (DOS) and transport distribution function of $BaFe_4Sb_{12}$, and (b) DOS for RFe_4Sb_{12} with divalent fillers. Zero energy points in both (a) and (b) are the maxima of valence bands. Unit for DOS is states/(eV cell). Group velocity **v** is in the unit of $m \cdot s^{-1}$.

R-Sb distances, which are clearly different among Ca-, Sr-, and Ba-filled RFe_4Sb_{12} (Table I).

Similar with the three AE-filled RFe_4Sb_{12}, we find notable differences between the band structures of $NaFe_4Sb_{12}$ and that of KFe_4Sb_{12}. The RFe_4Sb_{12} with trivalent rare earth fillers usually have very small Δ_0, which is the distinct feature of these systems and probably reflects the dependence of bands on the charge states of the fillers through the Coulomb potential. Interestingly, the details of the band structures of $YbFe_4Sb_{12}$ and $CaFe_4Sb_{12}$ around Fermi levels are relatively similar. This fact indicates again that the atomic size and charge state of a filler are the key factors in determining band details, since the Ca and Yb share similar atomic sizes and charge states, but differ in other aspects, such as electronegativity (1.0 vs 1.1) and orbital structure (electrons from 4*s* vs 6*s* states).

The density of states $N(E)$ and transport distribution functions $N(E)\langle \mathbf{v}^2 \rangle$ were also calculated. These are directly related to the electrical transport properties. Figure 3(a) shows the DOS and transport distribution function of *p*-type $BaFe_4Sb_{12}$, taking the energy zero at the VBM. The light band has a very small contribution to the DOS, reflected in the very small DOS values over the range −0.25–0 eV in Fig. 3(a). In the transport distribution function, $N(E)\langle \mathbf{v}^2 \rangle$, which weights the dispersive light band more greatly than the $N(E)$, the contribution of the light band is still small [Fig. 3(a)]. Furthermore, the Fermi level is over 0.2 eV lower than the onset of the heavy bands, making the light band even less important for the electrical transport, since only states within several k_BT around the Fermi level contribute significantly to electrical transport. These results suggest the electrical properties of $BaFe_4Sb_{12}$ and other RFe_4Sb_{12} are mainly affected by the heavy bands in VB. Figure 3(b) gives the comparison of DOS among RFe_4Sb_{12} with divalent fillers. Due to the variations in band structures, the RFe_4Sb_{12} with different filler atoms have some differences in the valence band DOS. Each system has a very low DOS ranging from about −0.2 eV to 0, reflecting the energy range of the light band. The DOS of the Ca- and Yb-filled RFe_4Sb_{12} are sharply increasing almost at the onset of their heavy bands, at about 0.16–0.18 eV below VBM in Fig. 3(b). In contrast to the two cases, the DOS slope of $BaFe_4Sb_{12}$ is relatively low after the energy of Δ_0, then becomes enhanced and comparable to $CaFe_4Sb_{12}$ after another energy of Δ_1 (0.12 eV). The results of $SrFe_4Sb_{12}$ fall in between those of the Ba- and Ca-, Yb-filled RFe_4Sb_{12}. As mentioned in band structures, the Δ_1 values of $CaFe_4Sb_{12}$ (0.03 eV), $SrFe_4Sb_{12}$ (0.08 eV), and $BaFe_4Sb_{12}$

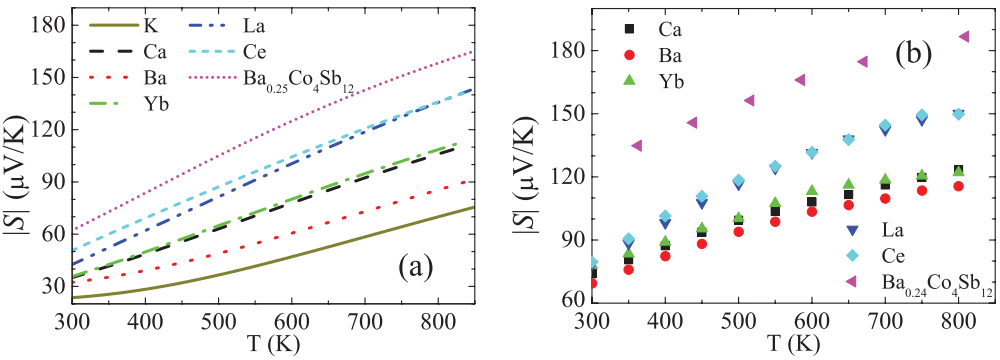

FIG. 4. (Color online) (a) Theoretical and (b) experimental temperature dependence of Seebeck coefficients for RFe_4Sb_{12}. Results for Ba-filled *n*-type $CoSb_3$ (negative Seebeck) are also shown for comparison.

(0.12 eV) show an obvious increasing tendency, causing the DOS variations since the energy pocket along H → N is an effective DOS contributor. Thus, one may anticipate that the Seebeck coefficients for $BaFe_4Sb_{12}$ and $SrFe_4Sb_{12}$ will be lower than those of $CaFe_4Sb_{12}$ or $YbFe_4Sb_{12}$.

IV. ELECTRICAL TRANSPORT PROPERTIES

A. Seebeck coefficient

The temperature dependence of Seebeck coefficients for several RFe_4Sb_{12} is calculated and shown in Fig. 4(a), together with the experimental results for RFe_4Sb_{12} with trivalent and divalent fillers [Fig. 4(b)].[24] The approach of calculations has been applied in understanding the electrical transport properties of n-type filled skutterudites.[15] When comparing the electrical transport properties from first-principles calculations with experimental results, the general trends of electrical transports instead of the exact agreement between the obtained values should be more emphasized because of a few uncertainties, such as experimental conditions of synthesis and measurements, possible filling deficiency in $R_xFe_4Sb_{12}$, and some physically sensible but not exact theoretical approximations. Overall speaking, the calculated Seebeck coefficients agree reasonably well with experiments, especially at high temperature. Since all the compounds are heavily doped semiconductors with band gaps no less than 0.5 eV, the Seebeck coefficients keep increasing in the temperature range of 300–850 K, and bipolar effect is not notable in either calculations or experiments.

The charge state of the fillers determines the free carrier concentration and band filling and therefore is the critical factor in determining the Seebeck coefficients. The RFe_4Sb_{12} with trivalent fillers possesses one hole per unit cell and shows relatively high Seebeck coefficients, about 135 μV/K at 850 K in calculations; RFe_4Sb_{12} with divalent fillers, about 90–110 μV/K, and monovalent fillers, about 75–90 μV/K. However, even for the systems with trivalent fillers, their Seebeck coefficients in both theory and experiment are still not sufficiently high for prominent performance. In fact, by using the Wiedemann–Franz relation $\kappa_e = L\sigma T$ and rewriting the TE figure of merit as $ZT = rS^2/L$ with $r = \kappa_e/(\kappa_e + \kappa_L)$ being lower than unity, the upper limit of a materials could be estimated as $(ZT)_{\max} \sim S^2/L$. The L is the Lorentz number for the material, typically not far from the value $L_0 = 2.0 \times 10^{-8}$ V^2/K^2 in degenerate semiconductors. $S \sim 160$ μV/K is required for $ZT = 1$ under the best scenario with a negligible κ_L. The overly p-type band filling is the origin of the relatively low Seebeck coefficient and thus the low electrical performance of RFe_4Sb_{12}. Seebeck coefficients of these p-type skutterudites need to be substantially increased to match the performance of the best n-type skutterudites, which requires lower hole concentrations, i.e. higher electron counts.

To emphasize the difference from n-type materials, the Seebeck coefficient and its temperature dependence of a partially Ba-filled n-type $CoSb_3$ skutterudite are also shown in Fig. 4. Theoretical values are from our previous calculation,[15] and the experimental values are from Chen *et al.*[8] When the electron concentrations are close to 0.5 electrons per Co_4Sb_{12} cell as in the case of $Ba_{0.25}Co_4Sb_{12}$, the absolute Seebeck coefficients could reach 170 μV/K at elevated temperature. In this regard, for the fully filled compounds RFe_4Sb_{12}, it is impossible to enhance the Seebeck coefficient to very high values with only the monovalent, divalent, or trivalent fillers.

Fillers may also have influences on Seebeck coefficients among the same band-filling compounds due to the electronic structure variations. In general, the calculated Seebeck coefficients of $LaFe_4Sb_{12}$ and $CeFe_4Sb_{12}$ are very close to each other, consistent with experiment. This can be explained by the similar valence band DOS (not shown) of the two compounds. The four divalent fillings, however, show noticeable diversions in Seebeck coefficients from our calculations. Ca- and Yb-filled RFe_4Sb_{12} show similar Seebeck coefficients over the whole temperature range, in accord with their similar band structures and DOS [Fig. 3(b)]. However, in theory, $BaFe_4Sb_{12}$ has lower Seebeck coefficient than the other divalent fillings, which is consistent with the relatively weaker energy dependence of DOS as shown in Fig. 3(b). In experiments, the Ba-filled system does show slightly lower Seebeck coefficient than the other systems with divalent fillers, but the strength is not as large as theoretically predicted, probably due to the difference in filling fractions.

B. Electrical conductivity

While the Seebeck coefficient of a material is given without adjustable parameters in Boltzmann theory with the constant relaxation time approximation, the electrical conductivity σ

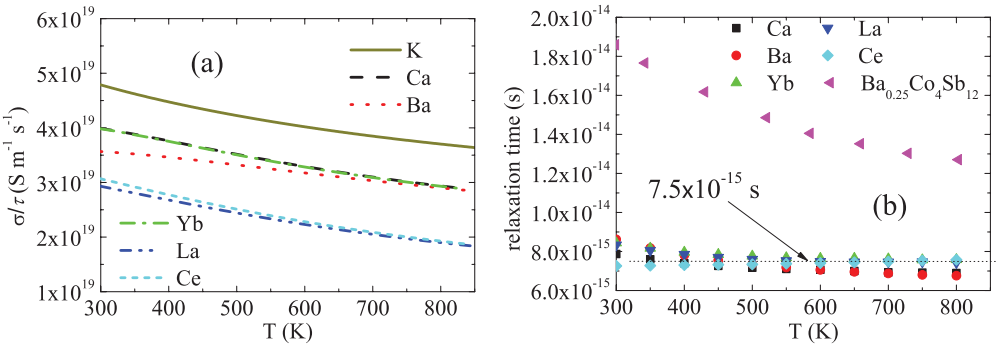

FIG. 5. (Color online) (a) Theoretical electrical conductivities for several RFe_4Sb_{12}. (b) Extracted relaxation times for RFe_4Sb_{12} and one Ba-filled n-type skutterudite.

depends on the relaxation time τ, which cannot be determined from the band structure alone. Nevertheless, the calculated σ/τ, as shown in Fig. 5(a), are helpful in understanding the trends. Similar to the Seebeck coefficients, the calculated electrical conductivities strongly depend on the charge states of fillers controlling the band fillings and thus the Fermi levels. Monovalent fillers yield largest σ/τ, and trivalent fillers the lowest as may be anticipated. Surprisingly, the temperature dependences of theoretical σ/τ are very close to those of experimental σ for all $R\mathrm{Fe_4Sb_{12}}$.[24] By combining the calculated σ/τ with the measured σ, the carrier relaxation times (τ) could be estimated, and the results are shown in Fig. 5(b). Note that the resulting τ is only an effective parameter incorporating all scatterings in an average way, while in reality there may even be nontrivial momentum and energy dependence in multiband materials such as the p-type skutterudites. In any case, the τ of all the $R\mathrm{Fe_4Sb_{12}}$ fall within a small range, from (7–8.5) $\times 10^{-15}$ s at 300 K and (6.5–7.5) $\times 10^{-15}$ s at 800 K. The values are weakly dependent on the filler types and even not strongly correlated to the temperature. Overall, a constant value, $\sim 7.5 \times 10^{-15}$ s, can be used to roughly describe the relaxation time for all $R\mathrm{Fe_4Sb_{12}}$ in the whole temperature range. In Fig. 5(b), the τ of one Ba-filled n-type skutterudite is also given, extracted from the theoretical σ/τ of $\mathrm{Ba_{0.25}Co_4Sb_{12}}$ (Ref. 15) and experimental σ of $\mathrm{Ba_{0.24}Co_4Sb_{12}}$.[8] Over the same temperature range, as shown in Fig. 5(b), the variations of τ for n-type skutterudites are relatively large (from 1.9×10^{-14} s to 1.2×10^{-14} s) and show the expected $1/T$ trend due to electron-phonon scattering. The value of τ in n-type $\mathrm{Ba_{0.25}Co_4Sb_{12}}$ is substantially higher than those in the p-type $R\mathrm{Fe_4Sb_{12}}$.

In $R\mathrm{Fe_4Sb_{12}}$, the weak dependence of carrier relaxation time on temperature is quite interesting, as normally with such high carrier concentrations one may expect that the electron-phonon interaction would dominate carrier transport from room to elevated temperature, yielding a near linear temperature dependence of the scattering rate, τ^{-1}.[60,61] The scattering mechanism in $R\mathrm{Fe_4Sb_{12}}$ is possibly a mixture of the intrinsic electron-phonon scattering and some other scattering mechanisms. In terms of electron-phonon scattering, large DOS (or effective mass) around the Fermi levels increase the rate that carriers are scattered by phonons and thus cause weak temperature dependence of relaxation time.[60,61] In our calculations, although the band-edge characters in both VB and CB are mainly d states from TMs, the d bands in VB are more localized and may cause stronger electron-phonon scattering than CB bands. This may result in a much weaker temperature dependence of carrier relaxation time in p-type $R\mathrm{Fe_4Sb_{12}}$ as compared with that in n-type $\mathrm{CoSb_3}$ skutterudites. Regarding extrinsic mechanism, it is most likely that point defect scattering contributes the change of temperature dependence, and the deficiencies of void filling (less than 100% filling of R) in practice is likely to be the source of point defect scattering. Since the intrinsic electron-phonon scattering always exists, a possible approach in order to improve the electrical conductivity in $R\mathrm{Fe_4Sb_{12}}$ is to increase the filling fraction to unity and therefore to reduce the effect of point defect scattering on carrier transport. However, as mentioned above, the current materials have performance limited primarily by the low Seebeck coefficient rather than the resistivity. Further enhancement of ZT requires an effective strategy to increase the magnitude of Seebeck coefficients for all Fe-based skutterudites.

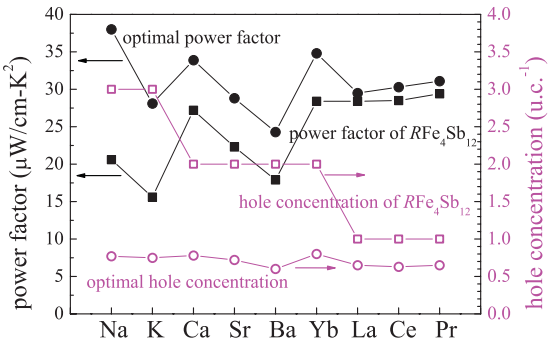

FIG. 6. (Color online) Power factors and hole concentrations (in unit of holes per unit cell) of $R\mathrm{Fe_4Sb_{12}}$. Maximum power factors and corresponding optimal hole concentrations are also given.

C. Power factor and optimization strategy

The power factors can then be obtained by using calculated $S^2\sigma/\tau$ and the estimated relaxation time (7.5×10^{-15} s). Figure 6 shows the exact values of power factors and hole concentrations at high temperature (850 K). Rigid band approximation is adopted in order to evaluate the maximum power factors and the corresponding optimal carrier concentrations of the $R\mathrm{Fe_4Sb_{12}}$. The hole concentrations for the fully stoichiometric monovalent, divalent, and trivalent fillings are three, two, and one hole per $R\mathrm{Fe_4Sb_{12}}$ cell and will be higher if the filling fraction is less than unity. However, when maximizing the power factors, the optimal hole concentrations of all these compounds are within a small range, about 0.6–0.8 holes per $R\mathrm{Fe_4Sb_{12}}$ cell. All $R\mathrm{Fe_4Sb_{12}}$ possessing similar optimal hole concentrations testifies the fact that electrical transport of these compounds are mainly determined by the heavy bands. The actual optimal hole concentration for maximizing ZT may depend on the details of the scattering rates determining the κ_e and κ_L at those doping levels, but will certainly be at still lower hole concentration because κ_e must decrease with decreasing hole concentration. The optimal carrier concentration is therefore perhaps a little larger than that in n-type skutterudites, but crucially is unreachable in the framework of $R\mathrm{Fe_4Sb_{12}}$ p-type skutterudites.

The fact that all alkaline, alkaline earth, and rare earth metal filled $R\mathrm{Fe_4Sb_{12}}$ are overly p doped and their low electronic relaxation times make it difficult to further enhance power factor and ZT. One possible solution to get optimal doped in the formula $R\mathrm{Fe_4Sb_{12}}$ is to find fillers with +4 charge state. Thorium would be one candidate, although for other reasons it is probably not useful for practical applications. Figure 7 plots the band structures of $\mathrm{ThFe_4Sb_{12}}$. When the crystallographic voids are fully filled with Th, it is a typical semiconductor. Considering the inevitable deviation from full filling, it is very likely to be naturally p-type doped and to have carrier concentrations near the optimum, which would correspond to a filling fraction $x \sim 0.85$–0.9.

Another solution is double or even multiple TM substitution for Fe. The choice of TMs may cover Fe, Co, Ni, and elements

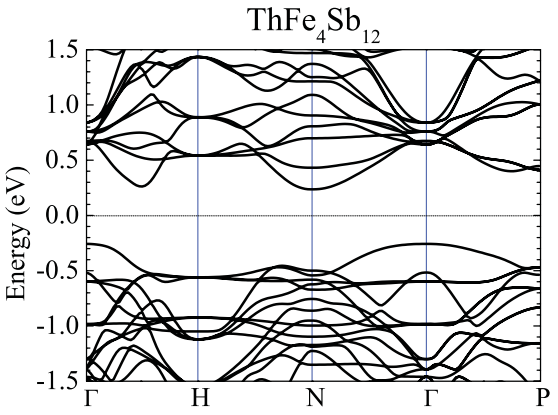

FIG. 7. (Color online) Band structures of $ThFe_4Sb_{12}$.

in the same columns of the periodic table. In fact, this has been explored particularly with Co, starting with the work of Sales *et al.*[2] In multiple TM substitution, the hole concentrations can be tuned using Fe-TM alloying. High Seebeck coefficients up to 170–180 μV/K can thus be achieved.[23,62] However, reported power factors in multiple transition metal substituted p-type skutterudites are even smaller than those of the RFe_4Sb_{12}. They are limited by two issues: large electrical transport scattering and severe bipolar effects. Due to the less charge compensation of multiple TM substitutions, the filling fractions of them are not as high as in the $R_xFe_4Sb_{12}$ case, which may cause larger point defect scattering. Meanwhile, substitution on TM sites may also cause alloy scattering and even nonuniform distributions of fillers. Bipolar effects make the Seebeck coefficients go downwards when T is higher than 700 K, which is unfavorable to high power factors and ZT values. Optimization in multiple TM-substituted p-type skutterudites is challenging work since the two issues need to be overcome and requires both theoretical and experimental efforts.

V. CONCLUSION

To summarize, electronic structures and electrical transport properties of p-type skutterudites RFe_4Sb_{12} were studied systematically. The fillers cover alkaline metals, alkaline earth metals, and rare earth metals. Both the valence and conduction bands are mainly derived from d states from Fe, with the exception of one single light band at the top of valence band. The d derived bands in valence band are so heavy that they are pinning the Fermi levels in them and mostly determine the electrical transport properties. The main variations in band structures come from the charge and size of the filler atoms. The charge of the filler atom determines the band filling and plays a large role in determining the relative position of the light band and heavy bands, with high charge bringing them into closest proximity. The atomic size also plays a significant role by changing the R-Sb distances. For example, there are noticeable differences between the electronic structure of $BaFe_4Sb_{12}$ and $CaFe_4Sb_{12}$, which lead to differences in the electrical transport properties. Our calculated Seebeck coefficients are in reasonable accord with existing experimental values, although analysis of the experimental data is complicated by, for example, incomplete filling. In all RFe_4Sb_{12}, we find that the ZT is limited by the Seebeck coefficient, which is hardly over 140 μV/K. Electrical conductivities are also mainly determined by the charge states of fillers. Remarkably, comparison with experimental data shows weak temperature dependence, and the mechanism besides electron-phonon scattering is likely to be point defect scattering. The average carrier relaxation time of RFe_4Sb_{12}, 7.5×10^{-15} s, is much lower than those in n-type filled skutterudites. The optimal p-type doping levels for power factors are estimated to be 0.6–0.8 holes per unit cell. Since this hole concentration is unattainable in pure $R_xFe_4Sb_{12}$, future work aimed at increasing ZT should focus on the transition metal alloying and on reducing scattering of conducting carriers.

ACKNOWLEDGMENTS

This work is in part supported by National Basic Research Program of China (No. 2007CB607500), National Natural Science Foundation of China (Grant Nos. 11004210, 50825205, 51028201, and 50821004), Science Foundation for Youth Scholar of State Key Laboratory of High Performance Ceramics and Superfine Microstructures (No. SKL201004). Work at Oak Ridge National Laboratory is supported by the Department of Energy, Office of Basic Energy Sciences as part of the S3TEC Energy Frontier Research Center.

*wqzhang@mail.sic.ac.cn

[1] C. Uher, *Thermoelectric Handbooks: Macro to Nano*, edited by D. Rowe (CRC Press, New York, 2006), Chap. 34, pp. 34-1–34-17.
[2] B. C. Sales, D. Mandrus, and P. K. Williams, Science **272**, 1325 (1996).
[3] G. A. Slack and V. G. Tsoukala, J. Appl. Phys. **76**, 1665 (1994).
[4] J. Yang, D. T. Morelli, G. P. Meisner, W. Chen, J. S. Dyck, and C. Uher, Phys. Rev. B **67**, 165207 (2003).
[5] G. A. Lamberton Jr., S. Bhattacharya, R. T. Littleton IV, M. A. Kaeser, R. H. Tedstrom, T. M. Tritt, J. Yang, and G. S. Nolas, Appl. Phys. Lett. **80**, 598 (2002).
[6] G. J. Long, R. P. Hermann, F. Grandjean, E. E. Alp, W. Sturhahn, C. E. Johnson, D. E. Brown, O. Leupold, and R. Rüffer, Phys. Rev. B **71**, 140302(R) (2005).
[7] M. Puyet, B. Lenoir, A. Dauscher, P. Pécheur, C. Bellouard, J. Tobola, and J. Hejtmanek, Phys. Rev. B **73**, 035126 (2006).
[8] L. D. Chen, T. Kawahara, X. F. Tang, T. Goto, T. Hirai, J. S. Dyck, W. Chen, and C. Uher, J. Appl. Phys. **90**, 1864 (2001).
[9] Y. Z. Pei, L. D. Chen, W. Zhang, X. Shi, S. Q. Bai, X. Y. Zhao, Z. G. Mei, and X. Y. Li, Appl. Phys. Lett. **89**, 221107 (2006).
[10] Y. Z. Pei, Jiong Yang, L. D. Chen, W. Zhang, J. R. Salvador, and Jihui Yang, Appl. Phys. Lett. **95**, 042101 (2009).
[11] X. Y. Zhao, X. Shi, L. D. Chen, W. Zhang, W. B. Zhang, and Y. Z. Pei, J. Appl. Phys. **99**, 053711 (2006).
[12] X. Y. Zhao, X. Shi, L. D. Chen, W. Zhang, S. Q. Bai, Y. Z. Pei, X. Y. Li, and T. Goto, Appl. Phys. Lett. **89**, 092121 (2006).
[13] X. Shi, W. Zhang, L. D. Chen, and J. Yang, Phys. Rev. Lett. **95**, 185503 (2005).

[14]X. Shi, Jiong Yang, J. R. Salvador, M. F. Chi, J. Y. Cho, H. Wang, S. Q. Bai, Jihui Yang, W. Zhang, and L. D. Chen, J. Am. Chem. Soc. **133**, 7837 (2011).
[15]Jiong Yang, L. Xi, W. Zhang, L. D. Chen, and Jihui Yang, J. Electron. Mater. **38**, 1397 (2009).
[16]S. Q. Bai, Y. Z. Pei, L. D. Chen, W. Zhang, X. Y. Zhao, and J. Yang, Acta Mater. **57**, 3135 (2009).
[17]X. Shi, H. Kong, C. P. Li, C. Uher, J. Yang, J. R. Salvador, H. Wang, L. Chen, and W. Zhang, Appl. Phys. Lett. **92**, 182101 (2008).
[18]W. Y. Zhao, P. Wei, Q. J. Zhang, C. L. Dong, L. S. Liu, and X. F. Tang, J. Am. Chem. Soc., **131**, 3713 (2009).
[19]S. Q. Bai, X. Y. Huang, L. D. Chen, W. Zhang, X. Y. Zhao, and Y. F. Zhou, Appl. Phys. A **100**, 1109 (2010).
[20]J. P. Fleurial, A. Borshchevsky, and T. Caillat, *Proceedings of the 15th International Conference of Thermoelectrics* (IEEE, New York, 1996), pp. 91–95.
[21]B. C. Sales, D. Mandrus, B. C. Chakoumakos, V. Keppens, and J. R. Thompson, Phys. Rev. B **56**, 15081 (1997).
[22]X. F. Tang, L. D. Chen, T. Goto, and T. Hirai, J. Mater. Res. **16**, 837 (2001).
[23]G. Rogl, A. Grytsiv, E. Bauer, P. Rogl and M. Zehetbauer, Intermetallics **18**, 57 (2010); G. Rogl, A. Grytsiv, P. Rogl, E. B. Kerber, M. Zehetbauer, and S. Puchegger, *ibid.* **18**, 2435 (2010).
[24]P. F. Qiu, J. Yang, R. H. Liu, X. Shi, X. Y. Huang, G. J. Snyder, W. Zhang, and L. D. Chen, J. Appl. Phys. **109**, 063713 (2011).
[25]V. V. Krishnamurthy, J. C. Lang, D. Haskel, D. J. Keavney, G. Srajer, J. L. Robertson, B. C. Sales, D. G. Mandrus, D. J. Singh, and D. I. Bilc, Phys. Rev. Lett. **98**, 126403 (2007).
[26]D. A. Gajewski, N. R. Dilley, E. D. Bauer, E. J. Freeman, R. Chau, M. B. Maple, D. Mandrus, B. C. Sales, and A. H. Lacerda, J. Phys.: Condens. Matter. **10**, 6973 (1998).
[27]N. R. Dilley, E. J. Freeman, E. D. Bauer, and M. B. Maple, Phys. Rev. B **58**, 6287 (1998).
[28]E. Bauer, St. Berger, A. Galatanu, Ch. Paul, M. Della Mea, H. Michor, G. Hilscher, A. Grytsiv, P. Rogl, D. Kaczorowski, L. Keller, T. Hermannsdörfer, and P. Fischer, Physica B **312**, 840 (2002).
[29]A. Leithe-Jasper, W. Schnelle, H. Rosner, R. Cardoso-Gil, M. Baenitz, J. A. Mydosh, Y. Grin, M. Reissner, and W. Steiner, Phys. Rev. B **77**, 064412 (2008).
[30]W. Schnelle, A. Leithe-Jasper, H. Rosner, R. Cardoso-Gil, R. Gumeniuk, D. Trots, J. A. Mydosh, and Y. Grin, Phys. Rev. B **77**, 094421 (2008).
[31]A. Leithe-Jasper, W. Schnelle, H. Rosner, M. Baenitz, A. Rabis, A. A. Gippius, E. N. Morozova, H. Borrmann, U. Burkhardt, R. Ramlau, U. Schwarz, J. A. Mydosh, Y. Grin, V. Ksenofontov, and S. Reiman, Phys. Rev. B **70**, 214418 (2004).
[32]E. Bauer, St. Berger, Ch. Paul, M. D. Mea, G. Hilscher, H. Michor, M. Reissner, W. Steiner, A. Grytsiv, P. Rogl, and E. W. Scheidt, Phys. Rev. B **66**, 214421 (2002).
[33]W. Schnelle, A. Leithe-Jasper, M. Schmidt, H. Rosner, H. Borrmann, U. Burkhardt, J. A. Mydosh, and Yu. Grin, Phys. Rev. B **72**, 020402(R) (2005).
[34]J. P. Perdew, K. Burke, and M. Ernzerhof, Phys. Rev. Lett. **77**, 3865 (1996).
[35]P. E. Blöchl, Phys. Rev. B **50**, 17953 (1994).
[36]G. Kresse and D. Joubert, Phys. Rev. B **59**, 1758 (1999).
[37]G. Kresse and J. Furthmüller, Phys. Rev. B **54**, 11169 (1996).
[38]D. Parker and D. J. Singh, Phys. Rev. B **82**, 035204 (2010).
[39]H. Wang, Y. Pei, A. D. LaLonde, and G. J. Snyder, Adv. Mat. **23**, 1366 (2011).
[40]Jiong Yang, H. M. Li, T. Wu, W. Zhang, L. D. Chen, and Jihui Yang, Adv. Funct. Mater. **18**, 2880 (2008).
[41]T. J. Scheidemantel, C. Ambrosch-Draxl, T. Thonhauser, J. V. Badding, and J. O. Sofo, Phys. Rev. B **68**, 125210 (2003).
[42]G. K. H. Madsen, J. Am. Chem. Soc. **128**, 12140 (2006).
[43]H. J. Monkhorst and J. D. Pack, Phys. Rev. B **13**, 5188 (1976).
[44]D. J. Singh and M. H. Du, Phys. Rev. B **82**, 075115 (2010).
[45]K. Yosida, *Theory of Magnetism*, (Springer-Verlag, Berlin, 1996), Sec. 14, pp. 201–220.
[46]D. J. Singh and I. I. Mazin, Phys. Rev. B **56**, R1650 (1997).
[47]L. Nordstrom and D. J. Singh, Phys. Rev. B **53**, 1103 (1996).
[48]D. Bérardan, C. Godart, E. Alleno, E. Leroy, and P. Rogl, J. Alloy Compd. **350**, 30 (2003).
[49]K. Nouneh, Ali H. Reshak, S. Auluck, I. V. Kityk, R. Viennois, S. Benet, and S. Charar, J. Alloy Compd. **437**, 39 (2007).
[50]C. S. Garde and J. Ray, Phys. Rev. B **51**, 2960 (1995).
[51]D. J. Singh, *Recent Trends in Thermoelectric Materials Research II, Semiconductors and Semimetals* Vol. 70, edited by T. Tritt (Academic Press, San Diego, 2001) Chap. 5, pp. 125–177.
[52]D. J. Singh and W. E. Pickett, Phys. Rev. B **50**, 11235 (1994).
[53]D. T. Morelli, T. Caillat, J. P. Fleurial, A. Borshchevsky, J. Vandersande, B. Chen, and C. Uher, Phys. Rev. B **51**, 9622 (1995).
[54]A. Zhou, L. S. Liu, C. C. Shu, P. C. Zhai, W. Y. Zhao, and Q. J. Zhang, J. Electron. Mater. **40**, 974 (2011).
[55]J. O. Sofo and G. D. Mahan, Phys. Rev. B **58**, 15620 (1998).
[56]P. Blaha, K. Schwarz, G. K. H. Madsen, D. Kvasnicka, and J. Luitz, *WIEN2k, An Augmented Plane Wave Plus Local Orbitals Program for Calculating Crystal Properties*, edited by K. Schwarz (Vienna University of Technology, Vienna, 2001).
[57]Y. H. Li, X. G. Gong, and S. H. Wei, Appl. Phys. Lett. **88**, 042104 (2006).
[58]Y. Z. Zhu, G. D. Chen, H. G. Ye, A. Walsh, C. Y. Moon, and S. H. Wei, Phys. Rev. B **77**, 245209 (2008).
[59]J. C. Smith, S. Banerjee, V. Pardo, and W. E. Pickett, Phys. Rev. Lett. **106**, 056401 (2011).
[60]B. R. Nag, *Electron Transport in Compound Semiconductors* (Springer-Verlag, Berlin, 1980).
[61]P. B. Allen, Phys. Rev. B **17**, 3725 (1978).
[62]R. H. Liu, J. Yang, X. H. Chen, X. Shi, L. D. Chen, and C. Uher, Intermetallics **19**, 1747 (2011).